A collinear ferrimagnetic model with spins aligned along the *b*-axis is supported by the magnetic diffraction pattern at 1.8 K. The four V^{4+} spins in the unit cell are arranged in a three-up, one-down configuration, as shown in **Fig. 4(c)**, consistent with earlier DFT results.[3] The spin structure between T_{C1} and T_{C2} that hosts a skyrmion phase is expected to be incommensurate, as indicated by various chiral compounds that exhibit skyrmion lattice phases. A recent small-angle neutron scattering (SANS) experiment reveals a magnetic propagation vector k = (0, 0.0081, 0) from a single crystal sample.[4] For such an extremely long period-modulated spin structure, the period or magnetic structure cannot be determined solely by conventional NPD. By combining the propagation vector obtained from the SANS experiment with the magnetic diffraction pattern, one can distinguish among candidate models and conclude that a cycloidal spin structure, with spins evolving in the bc-plane as illustrated in **Fig. 4(d)**, is present.

In this report, two applications of NPD in condensed matter research are summarized, demonstrating that neutron diffraction provides unique information not accessible through other experimental techniques. (Reported by Chin-Wei Wang)

This report features the works of Hung-Duen Yang and his collaborators published in Phys. Rev. B ***111****, 214418 (2025), and Phys. Rev. B* ***112****, 024441 (2025).*

ANSTO WOMBAT – High-Intensity Powder Diffractometer

- NPD
- Materials Science, Chemistry, Condensed-matter Physics

References

1. D. C. Kakarla, A. Tiwari, Y. H. Tseng, T. W. Yen, H. C. Wu, C. W. Wang, M.-J. Hsieh, J.-Y. Lin, A. Pal, C. Dhanasekhar, D. P. Gulo, H. L. Liu, H. D. Yang, Phys. Rev. B **111**, 214418 (2025).
2. T. W. Kuo, C. C. Chen, D. C. Kakarla, A. Tiwari, C. W. Wang, M. Gooch, L. Z. Deng, C. W. Chu, H. D. Yang, H. C. Wu, Phys. Rev. B **112**, 024441 (2025).
3. S.-H. Kim, P. S. Halasyamani, B. C. Mottot, R. Sechadri, M. A. Green, A. S. Sefat, D. Mandrus, Chem. Mater. **22**, 5074 (2010).
4. T. Kurumaji, T. Nakajima, V. Ukleev, A. Feoktystov, T. Arima, K. Kakurai, Yoshinori Tokura, Phys. Rev. Lett. **119**, 237201 (2017).

Neutron Reflectometry Probes Critical Interface Effects in Ferroelectric $Hf_{0.5}Zr_{0.5}O_2$ Films

The interfacial structure of ferroelectric $Hf_{0.5}Zr_{0.5}O_2$ thin films has been shown to strongly influence device performance.

Introducing Zr into HfO_2 thin films lowers the crystallization temperature for the ferroelectric orthorhombic phase and promotes robust ferroelectric properties. A team led by Miin-Jang Chen (National Taiwan University) and Tzu-Yen Huang (NSRRC) systematically investigated the depth-dependent structure of ferroelectric $Hf_{0.5}Zr_{0.5}O_2$ (HZO) thin films. HZO metal–ferroelectric–metal (MFM) devices with W electrodes were fabricated by atomic layer deposition using thermal (THE), plasma-assisted (PLA), and atomic layer annealing (ALA) processes, and their ferroelectric properties were evaluated.

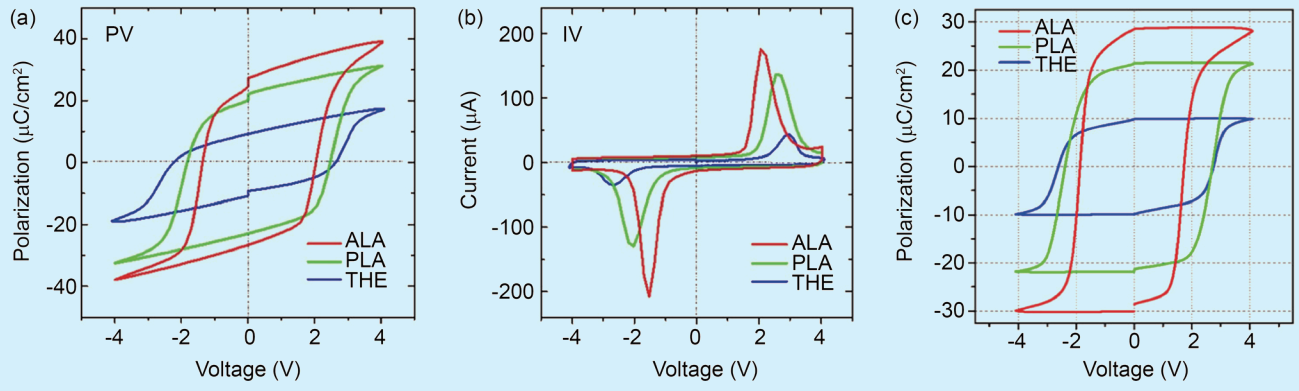

Fig. 1: (a) P–V hysteresis and (b) I–V switching responses show that the ALA device exhibits the largest Pr and the strongest switching current. (c) PUND-derived switching polarization measured with a 4 V pulse amplitude at 2 kHz confirms the most pronounced ferroelectric switching for the ALA-treated HZO film. [Reproduced from Ref. 1]

The team performed neutron reflectometry (NR) measurements on the **SPATZ** reflectometer at the Australian Nuclear Science and Technology Organisation (ANSTO) to probe buried interfaces in the HZO thin films.[1] **Figures 1(a) and 1(b)** show the polarization–voltage (P–V) hysteresis loops and current–voltage (I–V) switching characteristics of the THE, PLA, and ALA devices in the pristine state. Among these, the ALA device exhibits the largest remanent polarization (Pr) and the strongest switching current, indicating more pronounced ferroelectric switching in the ALA-processed HZO layer. **Figure 1(c)** displays the polarization switching extracted using the positive-up-negative-down (PUND) method. In this measurement, two consecutive positive pulses followed by two consecutive negative pulses are applied to isolate polarization switching while suppressing non-ferroelectric contributions, such as leakage- and capacitance-related currents, enabling a more reliable determination of 2Pr. The extracted 2Pr values are 57.9, 43.0, and 19.7 μC/cm^2 for the ALA, PLA, and THE devices, respectively. The highest 2Pr value observed for the ALA device suggests that the ALA treatment promotes a higher fraction of the ferroelectric orthorhombic phase in the HZO film, resulting in an enhanced ferroelectric response.

NR, with its high penetration depth, is well-suited for resolving the depth-dependent structure of MFM (W/HZO/W) devices and for probing buried interfaces that are challenging to access using other characterization techniques. **Figures 2(a)–2(c)** display the NR profiles for the THE, PLA, and ALA samples. The reflectivity data were analyzed using the *refnx* software,[2] where reasonable constraints were applied to the scattering length density (SLD) to ensure physically consistent refinement. The resulting fit curves show excellent agreement with the experimental data. The best-fit SLD depth profiles are summarized in **Fig. 2(d)**, highlighting distinct interfacial characteristics among the three processes.

For the THE sample, the HZO/W interfaces remain sharp, consistent with a well-defined heterointerface. The WO_X-related interfacial contributions extracted from the fits are sub-nanometer in thickness, indicating limited interdiffusion and minimal compositional grading at the HZO/W interface. By contrast, both PLA and ALA samples exhibit pronounced SLD gradients within the WO_X interfacial region, suggesting the formation of diffuse transition layers rather than an abrupt interface. Moreover, the WO_X interfacial layers in the ALA sample are thicker than those in the PLA sample. The fitted WO_X thicknesses near the top and bottom electrodes are 20 and 39 Å for the ALA sample, compared with 13 and 34 Å for the PLA sample. These results indicate stronger interfacial modification induced by the ALA treatment, potentially associated with elevated surface temperature during Ar plasma exposure. The fitted SLD values of the HZO layers are 5.5×10^{-6} Å^{-2}, 5.4×10^{-6} Å^{-2}, and 5.3×10^{-6} Å^{-2} for the ALA, PLA, and THE samples, respectively, indicating differences in film density and stoichiometry among the processes. The highest SLD observed for the ALA sample can be attributed to two factors: (1) additional Ar plasma exposure during ALA promotes film densification and improves crystallinity, and (2) the formation of a distinct WO_X interfacial layer at the bottom HZO/W interface, which can act as an oxygen reservoir during annealing. Such oxygen exchange can suppress oxygen-vacancy formation in HZO and thereby contribute to the increased SLD of the HZO layer in the ALA sample.

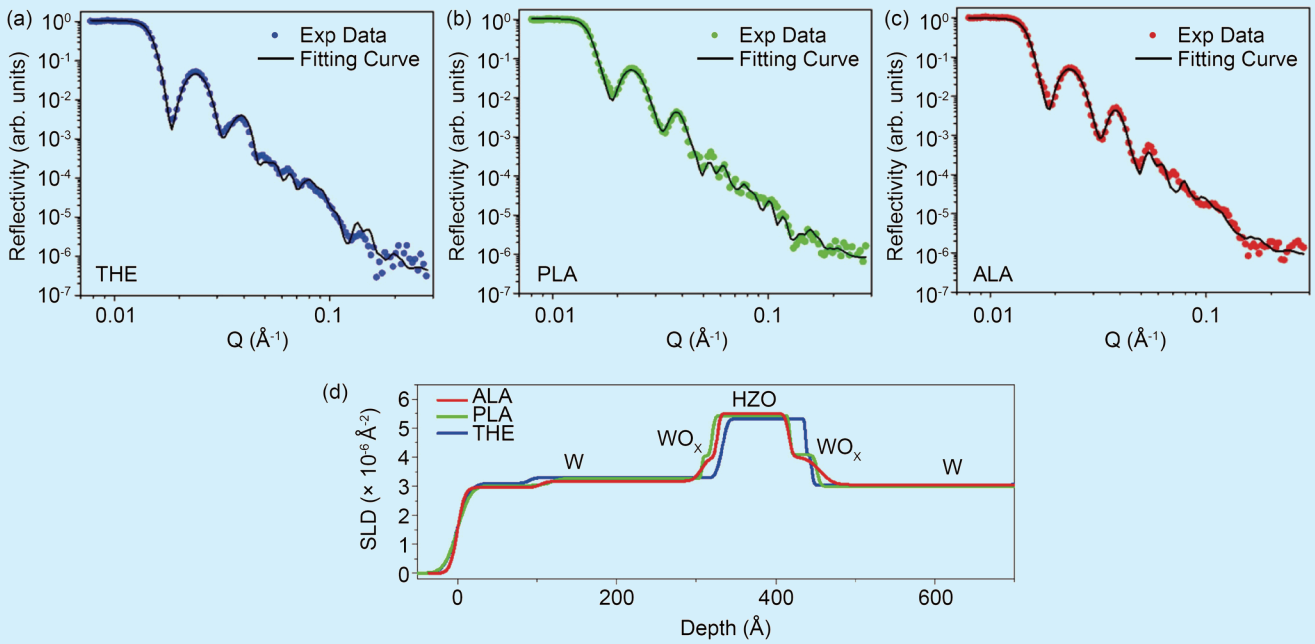

Fig. 2: NR profiles and fitting curves for HZO films prepared using (a) THE, (b) PLA, and (c) ALA methods. (d) Comparison of the corresponding SLD depth profiles extracted from reflectivity analysis. [Reproduced from Ref. 1]

In summary, this study used NR to investigate buried interfacial structures in W/HZO/W MFM devices composed of W, WO_X, and HZO layers. The NR analysis identified distinct bottom WO_X interfacial layers in the PLA and ALA samples, which can serve as oxygen reservoirs during annealing, suppressing oxygen-vacancy formation in HZO and stabilizing the ferroelectric orthorhombic phase. By contrast, the THE sample, fabricated without plasma treatment, exhibits weaker ferroelectric switching, consistent with a higher oxygen-vacancy concentration in the HZO film. Notably, the ALA treatment improves HZO densification and crystallinity and creates a more developed WO_X interfacial layer, resulting in the highest SLD and the strongest ferroelectric response. Overall, these findings provide a quantitative approach to resolving complex buried interface structures and emphasize the key role of interface engineering in enhancing HZO-based ferroelectric devices. (Reported by Tzu-Yen Huang)

This report features the work of Miin-Jang Chen and his collaborators published in ACS Appl. Mater. Interfaces ***17****, 16102 (2025).*

ANSTO SPATZ – Neutron Reflectometer

- NR
- Ferroelectric Thin Films, Atomic Layer Deposition and Interfaces

References

1. H. Y. Chen, C. L. Mo, J. J. Shyue, T. Y. Huang, M. J. Chen, ACS Appl. Mater. Interfaces **17**, 16102 (2025).
2. A. R. J. Nelson, S. W. Prescott, J. Appl. Crystallogr. **52**, 193 (2019).